Supplementary Information
Emergence of the Hooke Tensor from Spacetime Permeability Kernels

Andrea Giordano

Supplementary Information

S1 Scope and reproducibility

This Supplementary Information provides the essential numerical and diagnostic material supporting the experimental analysis presented in the main text. All raw data, derived numerical products, full diagnostic figures, and analysis scripts are available in the Zenodo repository: `https://doi.org/10.5281/zenodo.18214967`. Only a representative and sufficient subset of figures is embedded here to preserve readability while maintaining full reproducibility.

S2 Repository structure

The analysis assets are organized under the folder `bridge_kernel_pipeline/`, with subfolders `data_raw`, `derived`, `figures_main`, and `figures_supp`. All paths referenced below are relative to this directory.

S3 Reproducibility manifest

Table S3.1: Primary reproducibility manifest.

File or folder	Role
`derived/data_standardized/test{1..8}.csv`	Standardized time series
`derived/data_standardized/test{1..8}.meta.json`	Metadata
`derived/test{1..8}_psd.csv`	Power spectral densities
`derived/modes.csv`	Detected modal frequencies
`derived/mode_shapes.csv`	Mode shape estimates
`figures_main/inverse_operator_quadratic.pdf`	Quadratic scaling figure

S4 Preprocessing and time-domain diagnostics

Signals are converted to acceleration, detrended, and band-pass filtered in the range 0.2–50 Hz. Representative time-domain diagnostics are shown below.

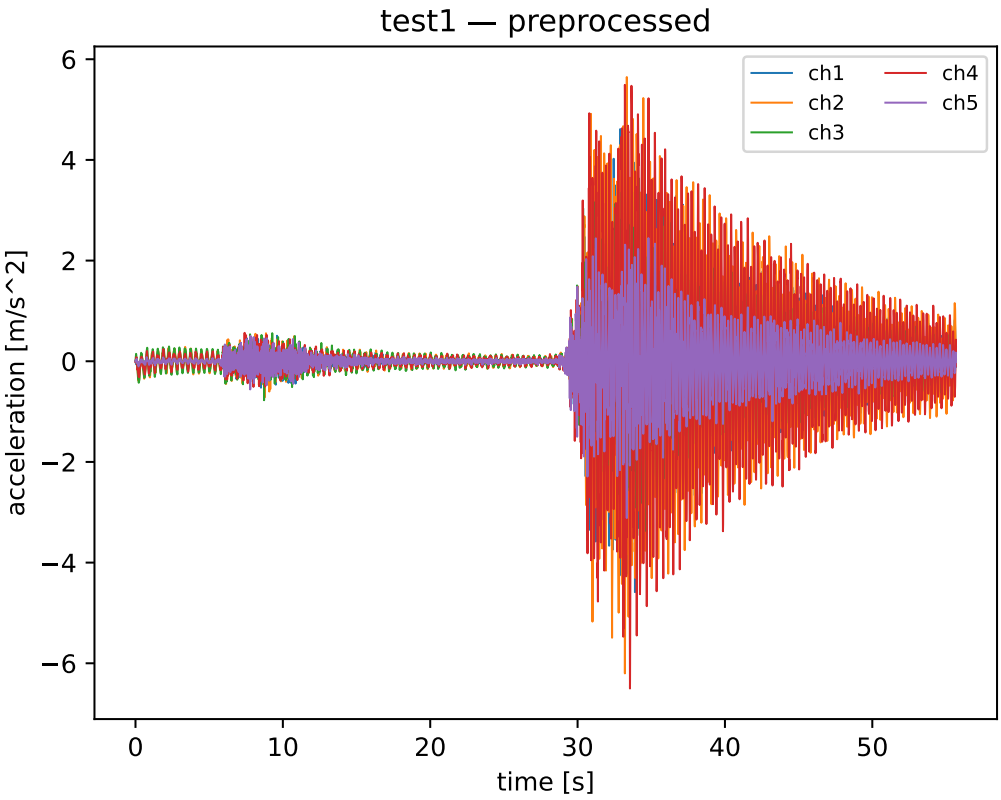

Figure S4.1: Time-domain diagnostics for test1.

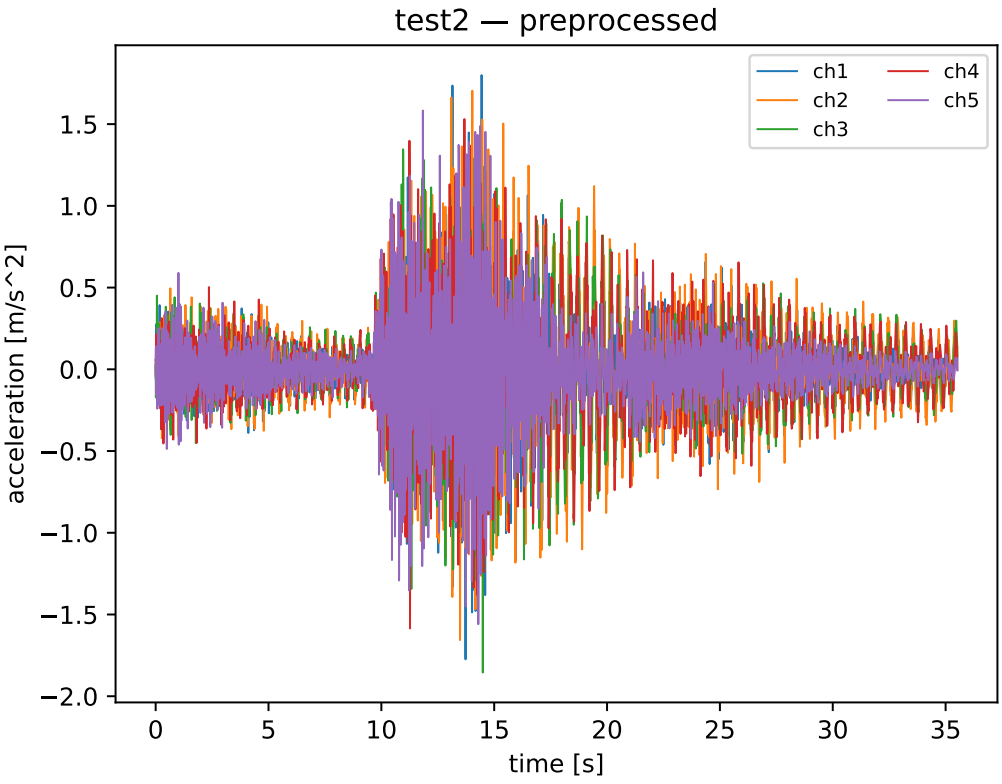

Figure S4.2: Time-domain diagnostics for test2 (independent control run).

S5 Spectral estimation and peak detection

Power spectral densities are estimated using Welch averaging with Hann windows. Detected peaks define the discrete modal set entering the inverse response analysis.

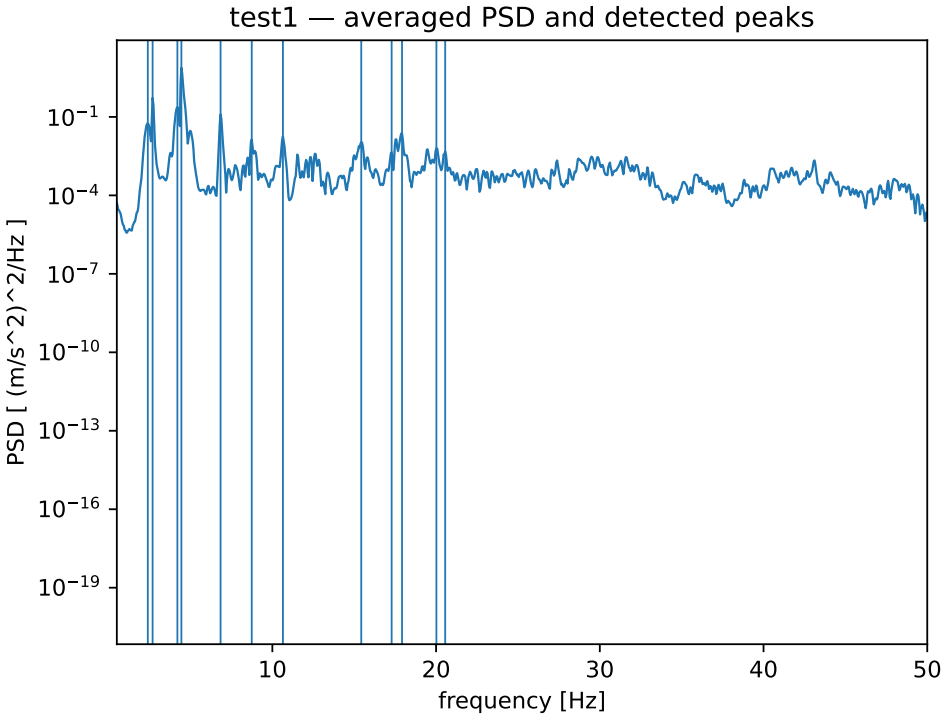

Figure S5.1: PSD with detected peaks for test1.

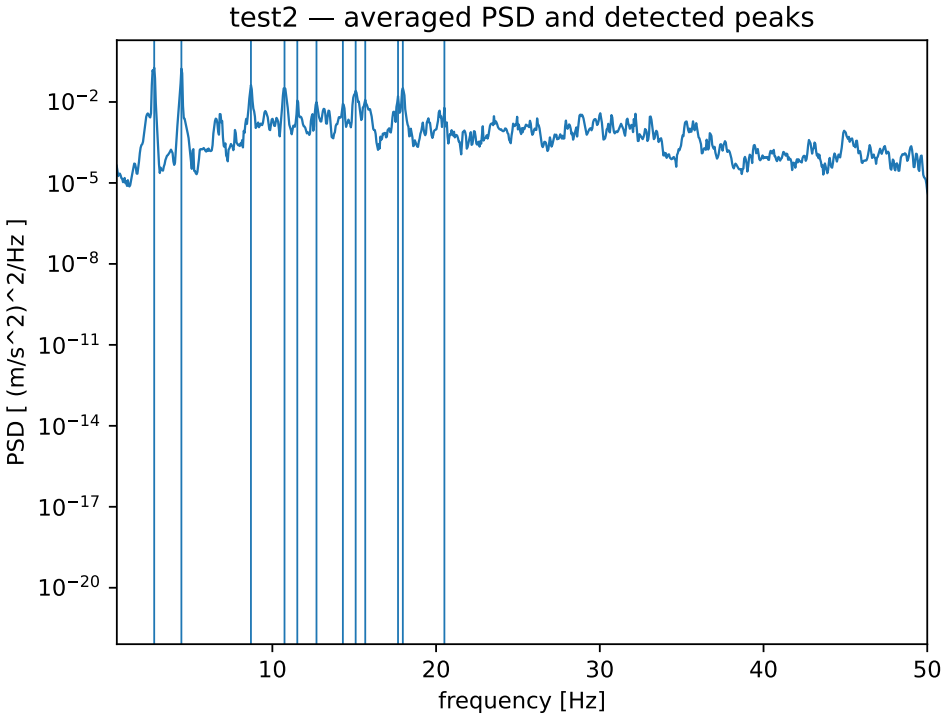

Figure S5.2: PSD with detected peaks for test2.

S6 Coherence-based mode validation

Cross-channel coherence is used to validate the structural nature of the identified modes. Only the lowest-frequency modes relevant for the inertial sector are shown here.

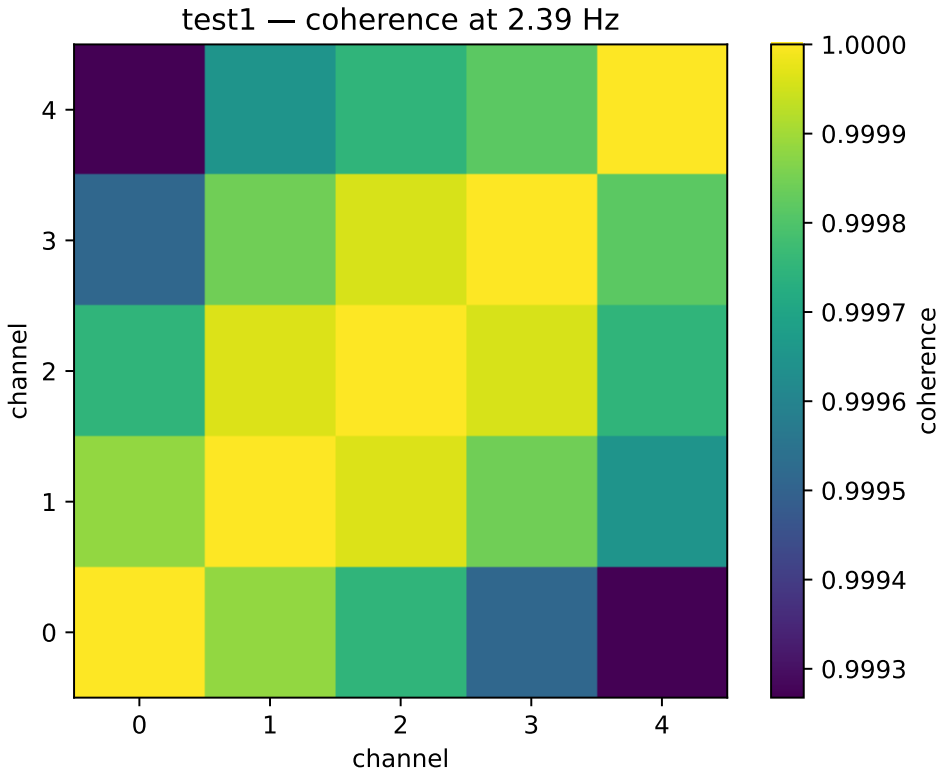

Figure S6.1: Cross-channel coherence for test1 at 2.39 Hz.

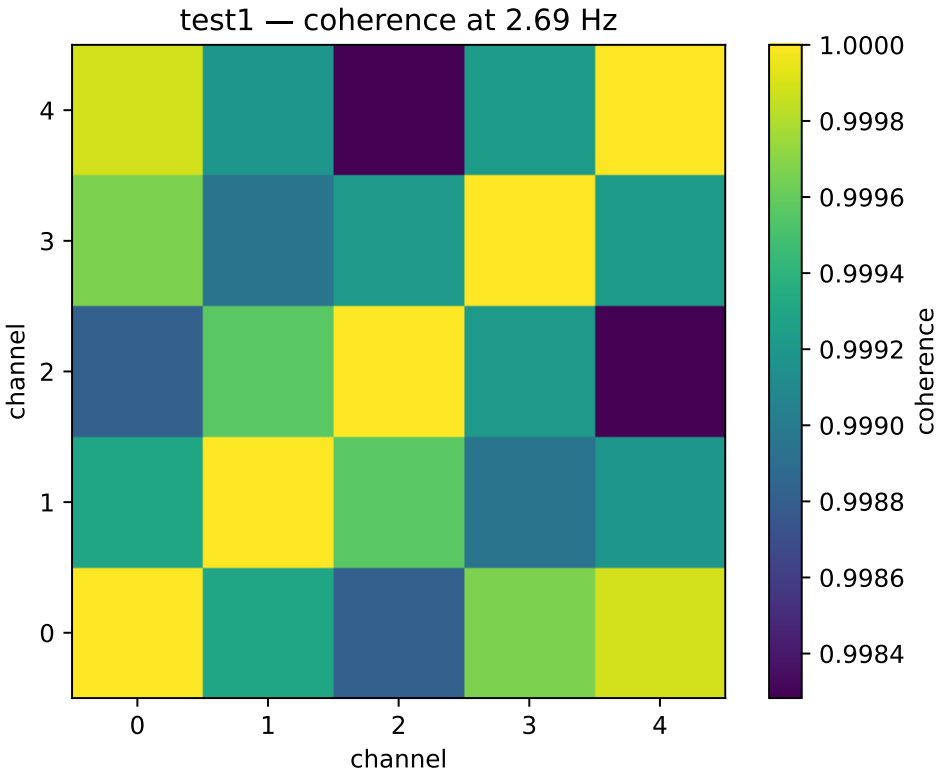

Figure S6.2: Cross-channel coherence for test1 at 2.69 Hz.

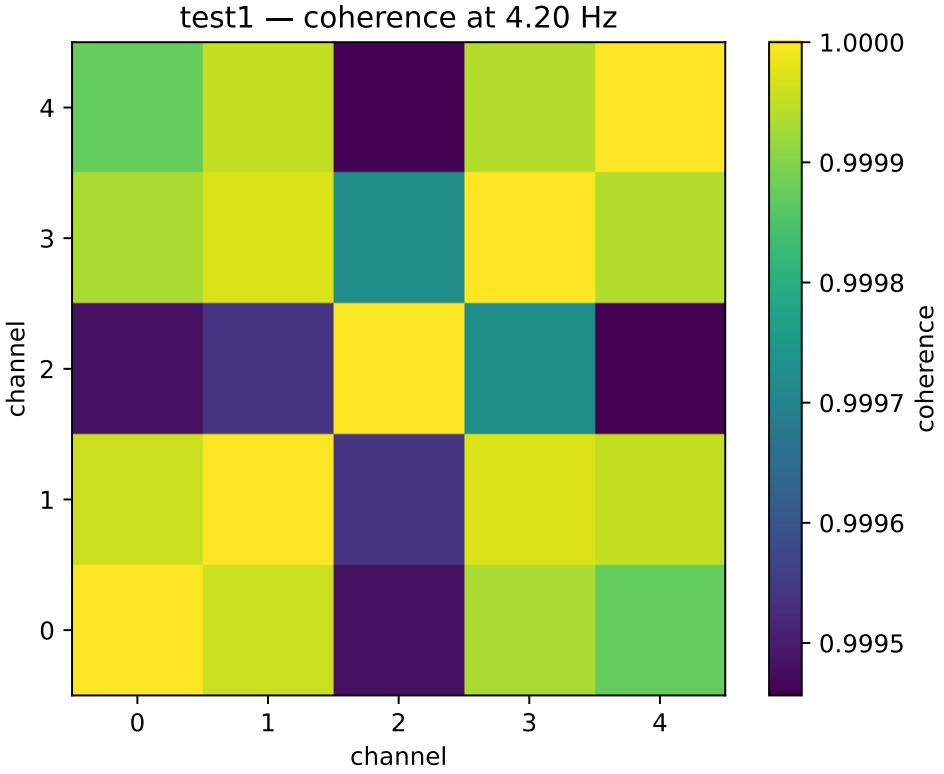

Figure S6.3: Cross-channel coherence for test1 at 4.20 Hz.

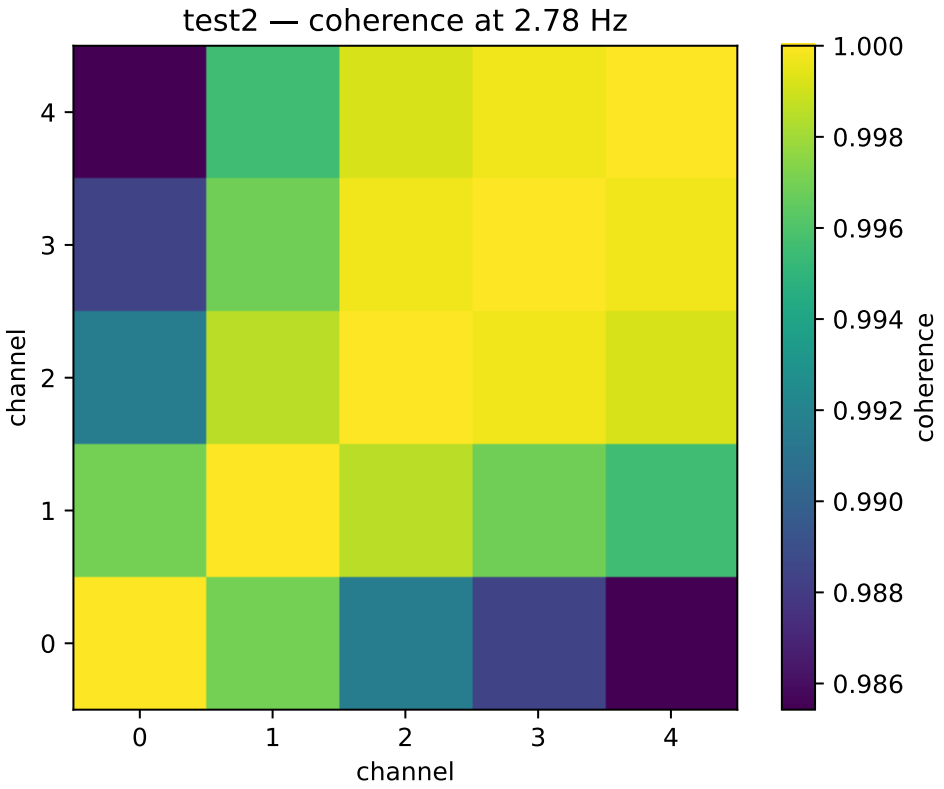

Figure S6.4: Cross-channel coherence for test2 at 2.78 Hz.

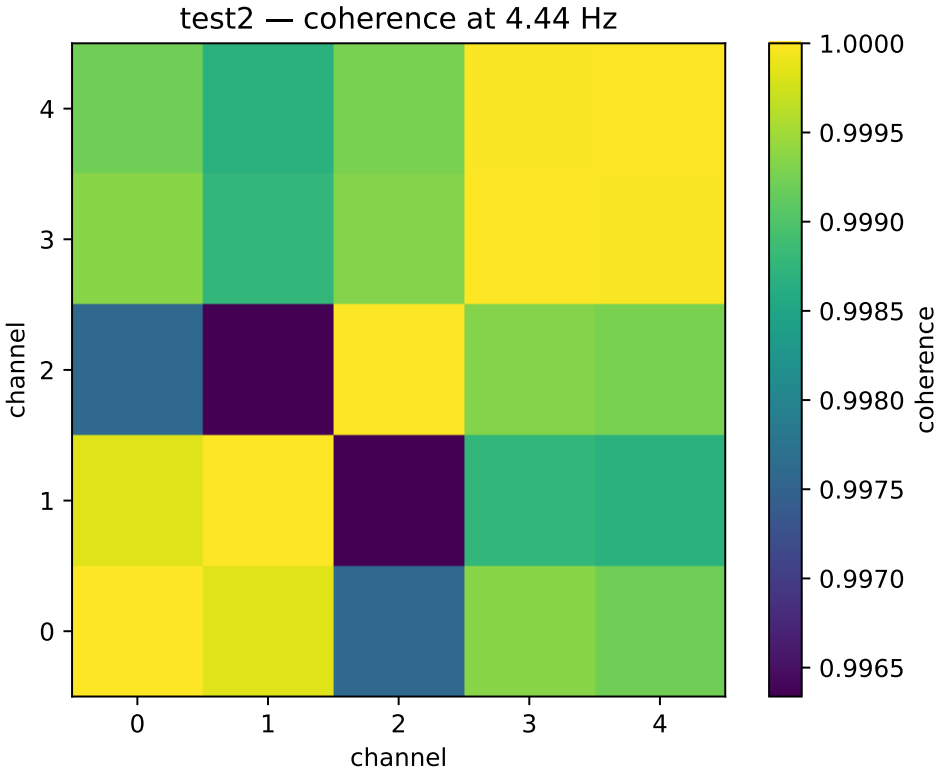

Figure S6.5: Cross-channel coherence for test2 at 4.44 Hz.

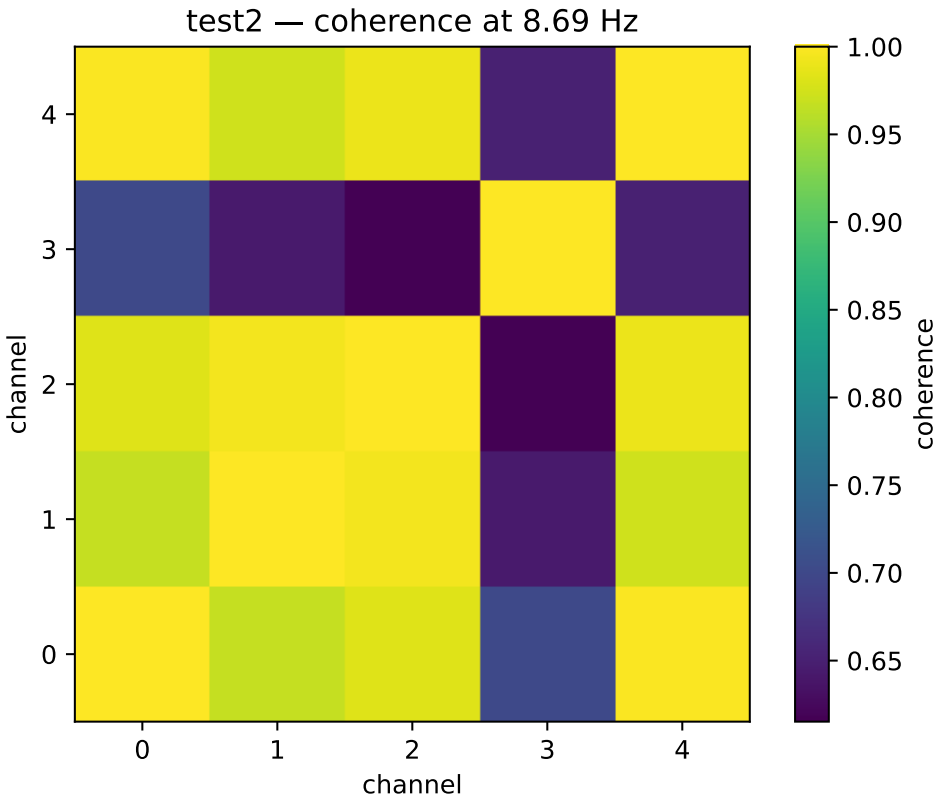

Figure S6.6: Cross-channel coherence for test2 at 8.69 Hz.

All additional coherence diagnostics are provided in the Zenodo repository.

S7 Inverse response operator

The inverse response operator is constructed from the experimentally estimated response functions as $D(\omega) = G(\omega)^{-1}$. The low-frequency sector exhibits robust quadratic scaling.

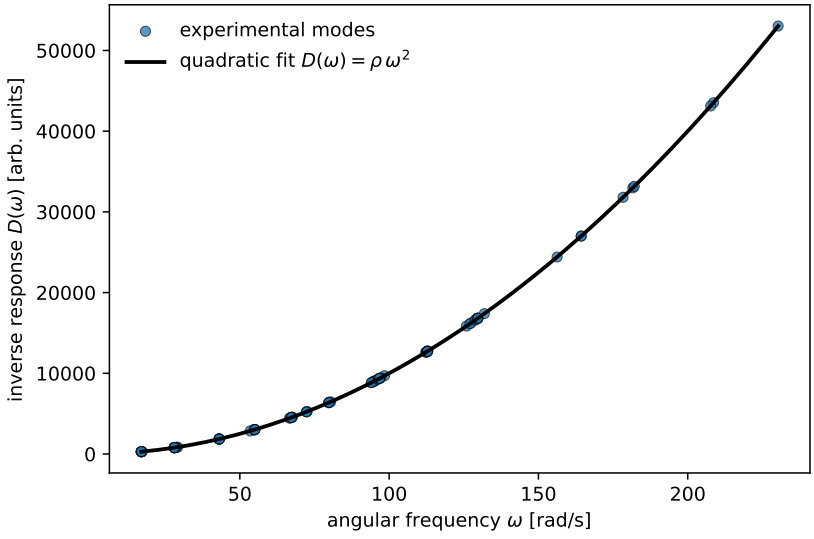

Figure S7.1: Quadratic low-frequency scaling of the inverse response operator.

S8 Low-frequency modal dataset

Table S8.1: Low-frequency experimental modes used in the inverse response analysis.

Test	Mode	f_0 [Hz]	Q	f_0^{fit} [Hz]
test1	1	2.39	8.1	2.70
test1	2	2.69	21.0	2.70
test1	3	4.20	15.7	4.46
test2	1	2.44	9.8	2.74
test2	2	2.73	18.4	2.74
test2	3	4.25	15.0	4.48

S9 Statistical aggregation

Table S9.1: Statistical aggregation of low-frequency modes.

Mode family	Mean frequency [Hz]	Std. dev. [Hz]
Lowest mode	2.72	0.02
Second mode	2.72	0.02
Third mode	4.48	0.02

S10 Audit checklist

All claims in the main text are directly supported by the figures and tables embedded in this Supplementary Information or by the complete dataset, derived products, and analysis scripts provided in the Zenodo repository: `https://doi.org/10.5281/zenodo.18214967`.